Three-Dimensional Refraction/Diffraction of Electromagnetic Waves Through Rocket Exhaust Plumes

A.J. Senol* and G.L. Romine†
Martin Marietta Corporation, Denver, Colorado

An analytical model has been developed to define the adverse effects that missile exhaust plumes have on radio communications with the missile. The computational model, RD3D, describes the three-dimensional propagation of electromagnetic waves through an ionized plume by refraction, the formation of blackout or dead zones, and dual-path contributions by diffraction from the fields outside the dead zone to the missile. The model relies on highly refined computations of the nozzle and plume chemistry and flowfields to establish the electron density distributions in the plume. These distributions are collapsed to a closed-form plume model for use in RD3D, a technique that contributes to computational time savings and increased accuracy. Results show the distortion of an electromagnetic wave as it encounters the plume and the received signal strength at the missile antenna. In order to verify the model and the individual components, comparisons are made to a number of classical refraction and diffraction cases, subscale missile diffraction tests, and full-scale missile development flight data. Results indicate refraction plays only a minor role in the received signal strength, while diffraction around an opaque circular disk may closely approximate the final results for motor propellants having high alkali content.

Nomenclature

da, ds	= element of surface
$f(\theta)$	= curve-fitted variable
k	= complex wavenumber
K	= Boltzmann's constant
m_e	= electron mass
m	= molecular weight of exhaust gas
n	= complex index of refraction
$\boldsymbol{n}$	= surface normal vector
$n(\theta)$	= curve-fitted exponent
N_a	= Avagadro's number
Q_i	= electron-neutral collision cross section of each species
r	= polar (spherical) coordinate of position
$\boldsymbol{r}$	= position vector
r_{source}, r_s	= distance from nozzle exit plane to nozzle throat
$\boldsymbol{t}$	= unit transmission vector
T	= electron temperature
$\boldsymbol{u}$	= unit vector tangent to wavefront
U, G	= analytic complex wavefunctions
dv	= element of volume
X_i	= mole fraction of individual species
α	= attenuation coefficient
β	= phase coefficient
θ	= polar (spherical) coordinate of angle
λ	= wavelength
ν_c	= electron-neutral collision frequency, s^{-1}
$\rho(r,\theta)$	= plume mass density in polar coordinates r, θ
$d\sigma$	= element of arc length
ω	= angular frequency
ω_p	= plasma frequency
$\hat{(\ )}$	= unit vectors

Introduction

THE terms refraction and diffraction have been conveniently defined in branches of physics and engineering in reference to the propagation of waves. From the initial step taken by Huygens in the evolution of wave propagation theory, many formulations have been developed to explain the nature of propagation of electromagnetic (EM) waves in a physical system. A physical system of particular interest to the Peacekeeper (PK) development program is the effect of a missile plume on EM wave propagation to and from the missile. Throughout the many years of launch vehicle development, the effects of the ionized rocket exhaust plume on radio-frequency (RF) communications have been studied in great detail. Until recently, the techniques employed to study the effects of the missile plume on RF communications have been simple diffraction models such as the two-dimensional infinite strip diffractor, circular disk diffractor, and simple refraction techniques in order to obtain the received fields.

The received field intensity is the quantity of primary interest, while phase information is included as a constituent of the resultant received intensity. In the method chosen for this investigation, only the scalar amplitude of one transverse component of either the electric or magnetic field is considered. This approach entirely neglects the fact that the electric and magnetic components of the field vector are coupled through Maxwell's equations, but fortunately at the frequencies of interest, as will be shown, the scalar theory yields accurate results if the effective diffractor is large compared to the wavelength and the fields are observed away from the effective diffractor.

This paper presents an overview of the analytical and computational techniques employed in combining an analytical plume model together with a three-dimensional wave propagation model in order to develop the three-dimensional refraction/diffraction model, RD3D. Results will be presented for plume definition, classical refraction and diffraction cases, experimental diffraction cases, and comparison of the modeled predictions of received signal strength at the command frequency of 0.4165 GHz to actual Stage III PK flight test data.

Theory

Beginning with a closed-form analytical expression for the plume electron density, an expression for the complex index of refraction is determined. The results are then incorporated into a unique application of classical ray optics and scalar diffraction theory to the problem of missile exhaust effects on the EM wave propagation.

Presented as Paper 84-1967 at the 17th AIAA Fluid Dynamics, Plasma Dynamics and Lasers Conference, Snowmass, CO., June 25-26, 1984; submitted June 29, 1984; revision received April 19, 1985.

*Staff Engineer.
†Senior Staff Engineer. Senior Member AIAA.

In general, the model development is composed of three parts: 1) plume density and index of refraction definition of the missile exhaust plume that includes the effects of alkali metal contaminants in the propellant, nonequilibrium thermochemistry, and expansion into the plume from the nozzle boundary-layer flows; 2) classical refraction and wavefront construction; and 3) application of classical scalar diffraction formulism to obtain the received EM fields.

Plume Density and Index of Refraction Definition

In order to model refraction of ray packets in the ionized missile plume, the electron density distributions must be determined so that variations of the complex index of refraction in the ionized exhaust plume can be defined.

A series of computer codes are used to obtain the flowfield and chemical information. The primary chemical investigations for the PK Stage III propellant are made using chemistry modules in the Solid Performance Program (SPP).[1-3] Beginning with trace elements of sodium and potassium measured in the propellant, nonequilibrium chemistry was computed through the nozzle and into the plume. The asymptotically approached value of the electron mole fraction was 4.2×10^{-7} located 2 m downstream from the exit, with the dominant charged particles being e^-, Cl^-, and K^+.

The plume flowfield for the PK Stage III solid-propellant motor was calculated by the coupled, two-phase program PLUME. PLUME is the largest and most complex program in the plume interference prediction (PIP) series and gives detailed flowfield information for the supersonic, axisymmetric, two-phase flowfield with the effects of nozzle boundary-layer expansion included.[4] The case studied was for a vacuum plume without the boundary shocks or afterburning as seen at lower altitudes. Once this detailed analysis is completed, a closed-form expression for the mass density distributions is constructed to match the PIP generated plume.

In general, the plume mass density for the plume was found to be

$$\rho(r,\theta)=3.3952\times10^{-5}\frac{\cos^{n(\theta)}[\theta/f(\theta)]}{(r+r_{\text{source}})^2} \tag{1}$$

where r_{source} is the exit radius ($=-0.938854$ m), r the distance from the nozzle exit in meters, and θ the angle off the plume centerline.

The exponent n and variable f are functions of θ as follows:

$$\begin{aligned}
n(\theta) &= -0.7\theta+32.0 && 0<\theta\le20\\
&= 0.2\theta+14.0 && 20<\theta\le40\\
&= 0.5\theta+2.0 && 40<\theta\le60\\
&= 0.2333\theta+46.0 && 60<\theta\le90\\
f(\theta) &= 2.0 && 0<\theta\le85\\
&= -0.1\theta+10.5 && 85<\theta\le90
\end{aligned}$$

The resulting plume density contours are shown in Fig. 1 for the vacuum plume.

In an exhaust plume characterized by contours of constant mass density ρ, the plume particle number density can be expressed as a fraction of the plume mass density.[2] The collision frequency is also related to the particle number density, and in general is given by the relation,[2,5]

$$\nu_c=\sqrt{\frac{8KT}{\pi m_e}}\frac{N_a\rho}{m}\sum_i X_iQ_i(T) \tag{2}$$

From the expression for the collision frequency, the complex index of refraction can be determined and is given by[5,6]

$$n=\left[\left(1-\frac{\omega_p^2}{\nu_c^2+\omega^2}\right)+i\frac{\nu_c}{\omega}\left(\frac{\omega_p^2}{\nu_c^2+\omega^2}\right)\right]^{1/2} \tag{3}$$

and since ∇n is related to the plume density by

$$\nabla n=\frac{\partial n}{\partial\rho}\nabla\rho \tag{4}$$

the gradient of the index of refraction is also determined. If an axisymmetric definition of the plume density is specified, the gradient of the index of refraction expressed in spherical coordinates is

$$\nabla n=\rho\frac{\partial n}{\partial\rho}\left[-\frac{2}{(r+r_s)}\hat{r}+\left(\frac{1}{rc}\frac{\partial c}{\partial\theta}-\frac{2}{r(r+r_s)}\frac{\partial r}{\partial\theta}\right)\hat{\theta}\right] \tag{5}$$

where

$$c=3.3952\times10^{-5}\cos^{n(\theta)}[\theta/f(\theta)]$$

Classical Refraction and Wavefront Construction

The next step to obtain the general solution of refraction and diffraction through the ionized plume is the description of refraction from a scalar wave optics approach. The scalar wave optics can then be combined with the general diffraction theory to yield a more comprehensive analysis of electromagnetic wave propagation through ionized media.

The mechanics of refractive optics employed in RD3D are based on a plane, linearly polarized wave as the scalar solution to the problem of electromagnetic wave propagation through a linear, isotropic, homogeneous plasma. Although, by definition, a medium is homogenus and isotropic only if its properties are the same at any point in all directions and orientations, the complete solution to the wave equation can be constructed by a technique known as Eikonal approximation.[5,7] With this technique, wave packet propagation can be extended to absorbing and refractive media by simply replacing the index of refraction n by its complex analog.[7] The spatial solution of ray position can then be generated from the Eikonal equation,

$$\frac{dt}{d\sigma}=\frac{\nabla n\cdot u}{n}u \tag{6}$$

The Eikonal approximation is valid in instances where the index of refraction is not changing appreciably compared with

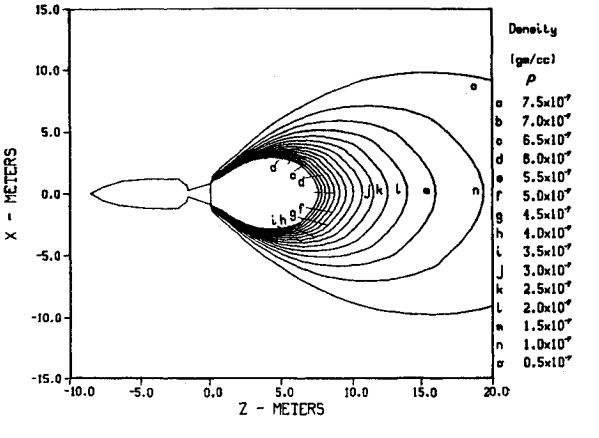

Fig. 1 Contours of constant density of the PK Stage III plume.

the wavelength.[7] Previous studies confirm the validity of the propagation techniques applied to the PK Stage III plume.[2] The Eikonal approximation to refractive optics is now coupled with the definition of the complex index of refraction to illustrate the propagation of EM waves through the PK Stage III plume. These refraction results were compared with a similar procedure in Ref. 8 and showed excellent agreement, thus validating the refraction formulation. Typically, individual ray packets are propagated from a point source on the missile in a piecewise manner described by standard propagation techniques.[7,8]

In Fig. 2, the two-dimensional downlink transmission of ray packets emanating from a point source on the missile is depicted from an angle of 90 to 0 deg, normal to and parallel to the missile axis, respectively. From this illustration, the formation of a "deadzone" or a region below which ray packets cannot propagate is easily seen. Figure 2 also illustrates a degenerate wavefunction of a position on a surface about a radiating source on the missile. This artifact is demonstrated in Fig. 3, where a summary of the total bending of each ray is given. Beyond the refractive plume and for transmission vector angles greater than the dead zone angle, the transmission vector angle θ_{out} can be generated from two independent incident ray packets at angles of θ_1 and θ_2 with respect to the missile axis. The dual-pathed wavefunction can be attributed to strong and weak refracted fields, depending on the history of the complex index of refraction through the missile plume.

In Fig. 4, an array of ray packets propagating uplink toward the missile also experiences a propagation "dead zone." From Figs. 2 and 4 it is easy to understand why earlier researchers modeled such physical systems as simple absorbing solid diffractors.[9-11]

Wavefront Construction

Program RD3D is based on formulations that require an intimate knowledge of the ray packet position history and the attenuation and phase coefficients on the surface of the propagating wavefronts in order to link scalar propagation theory with classical diffraction theory. By construction and generalization of the basic propagation formulism [Eqs. (6-13)], the solution to the wave equation (6) can be extended to three dimensions by noting that an element of the propagating surface is normal to the direction of propagation of the wave (i.e., the direction of the wave is the same as the direction of the transmission vector of a ray packet). A plane wavefront can then be constructed of a family of ray packets that initially lie in the same plane, have the same initial transmission vector, and have propagated by the same number of incremental steps into the plume.

To illustrate the deformation of a complete EM wave by the missile plume, an incoming plane wave was targeted to a point somewhat behind the missile nozzle. Typical wavefronts were generated and displayed by program RD3D. The particular example displayed in Fig. 5 represents the wavefunction of position of an incoming plane wave at the command frequency of 0.4165 GHz that encounters the PK Stage III exhaust plume at an angle of 30 deg to the missile axis. On all plots, the ionized exhaust plume extends along the $+Z$ axis with the nozzle located at the center of the X-Y plane.

As the plane wave is propagating toward the nozzle, particular attention should be paid to the "hole" that develops as the cutoff frequency limit is reached at that particular location in the plume. Areas of the plume having a large gradient of the index of refraction are identified by significant bending of individual ray packets.

Application of Classical Scalar Diffraction Theory to Obtain the Received Fields

Classical Formulism of Diffraction and RD3D

The primary foundation of scalar diffraction theory and the basis of RD3D is Green's theorem applied to complex wavefunctions of position. In the application of Green's theorem, the wavefunction and its normal surface gradient are solutions of the Helmholz equation or, in the application to inhomogeneous media, Helmholz manifolds.[12]

If U and G are two complex wavefunctions of position and S a closed surface surrounding a volume V, U and G and their

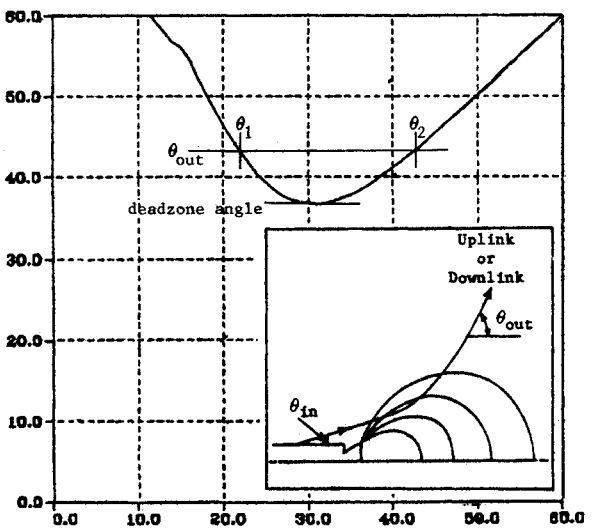

Fig. 3 Refraction histories of propagated downlink ray packets.

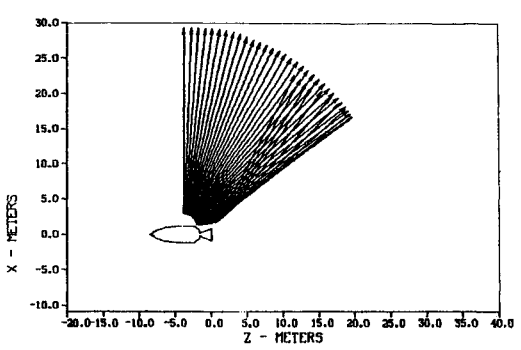

Fig. 2 Two-dimensional downlink transmission of ray packets from the vehicle at the command frequency of 0.4165 GHz.

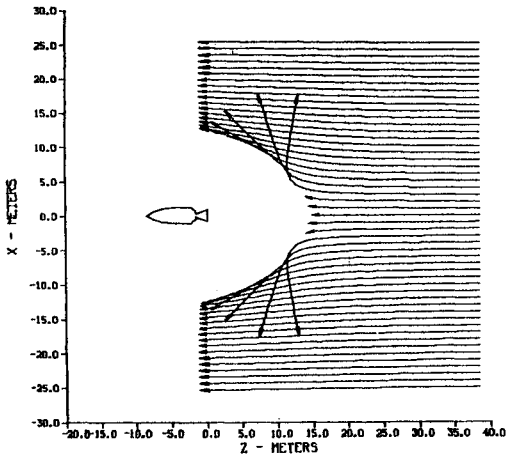

Fig. 4 Two-dimensional uplink transmission of ray packets from the vehicle at the command frequency of 0.4165 GHz.

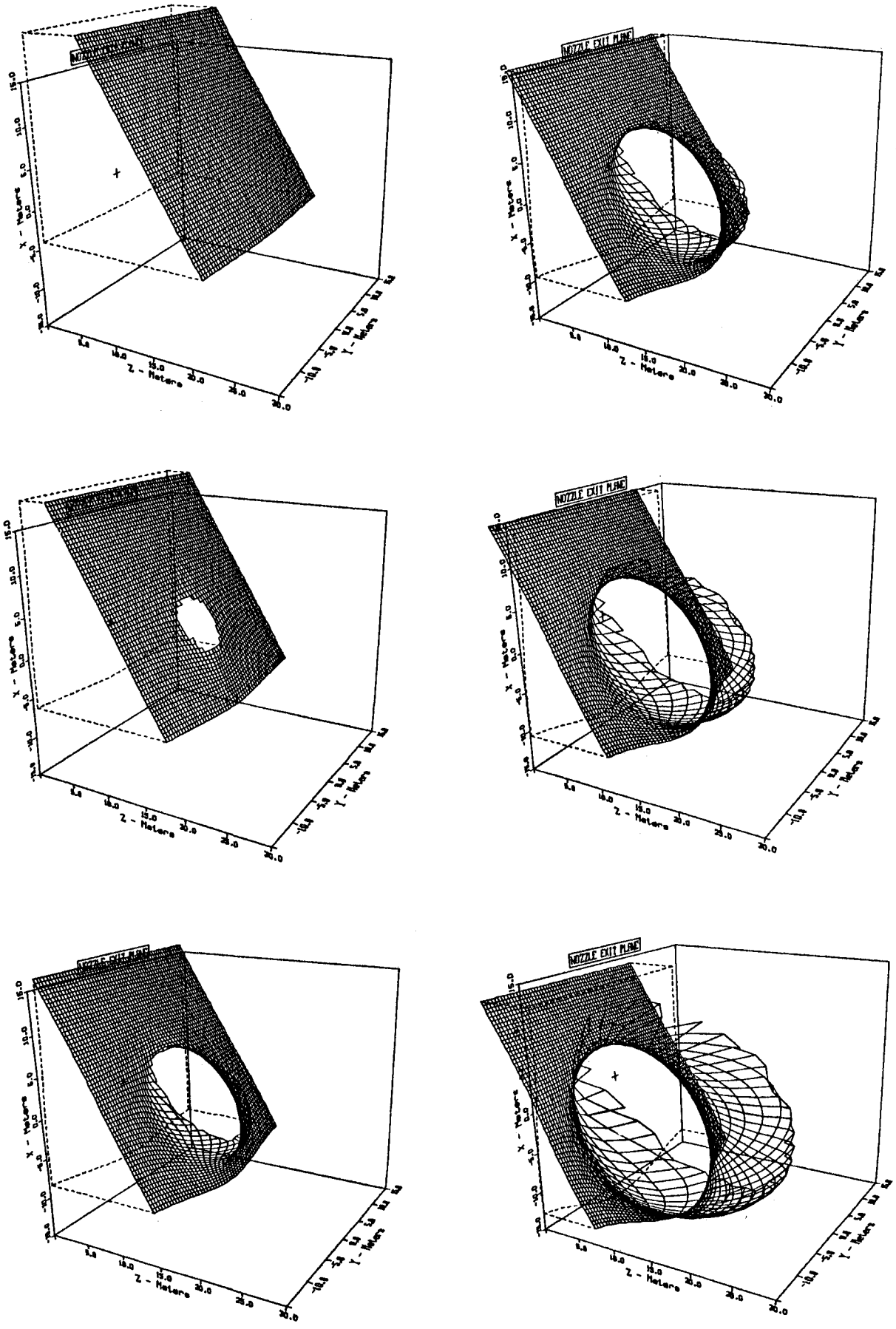

Fig. 5 Graphical depiction of the wavefunction of position during propagation of an EM wave through the missile plume at 30 deg aspect angle.

normal derivatives are continuous on the surface. Then,

$$\int_V (G\nabla^2 U - U\nabla^2 G)\mathrm{d}V = \int_S \left(G\frac{\partial U}{\partial n} - U\frac{\partial G}{\partial n}\right)\mathrm{d}a \qquad (7)$$

if G is taken to be the "free space" radiation function,

$$G = e^{ikr}/r \qquad (8)$$

The expression for the resultant complex field at a point P within the surface S can be found in many texts dealing with diffraction and advanced calculus and, in general, is[12-15]

$$U_p = \frac{1}{4\pi}\int_S \left[\frac{\partial U}{\partial n}\left(\frac{e^{ikr}}{r}\right) - U\frac{\partial}{\partial n}\left(\frac{e^{ikr}}{r}\right)\right]\mathrm{d}a \qquad (9)$$

This expression is particularly important as it allows the resultant field at the observation point P within the surface S to be determined solely by boundary conditions on the surface S. If U is the spherical wavefunction measured from the source, $\exp(ikr')/r'$, and the point of observation is many wavelengths from the diffractor such that

$$2\pi/\lambda \gg 1/r' \qquad (10)$$

the field at P can then be expressed as

$$U_p = \frac{-i}{4\pi}\int_S k\frac{e^{ik(r+r')}}{rr'}[\cos(n,r) - \cos(n,r')] + \frac{1}{rr'}e^{ik(r+r')}\left[\frac{\cos(n,r')}{r'} - \frac{\cos(n,r)}{r}\right]\mathrm{d}a \qquad (11)$$

where k is the complex wavenumber, r' the distance from the source to the diffractor, r the distance from the diffractor to the point of observation, and $\cos(n,r)$ the cosine of the angle subtended between the surface normal n and the vector r.

This expression, commonly referred to as the Fresnel-Kirkoff approximation, is the basis for the numerical computation of the net received EM field in program RD3D.[12-14]

Terms of Eq. (11) represent the illumination of a known surface S by a spherically expanding wave from a point source P' and the reradiation of elemental Huygens wavelets on the surface to an observation point P (Fig. 6).

In program RD3D, the Fresnel-Kirkoff approximation is interpreted as the illumination of a known surface S of a numerically generated and propagated uplink plane wave composed of elemental ray packets. The ray packet information containing the amplitudes of the complex wavefunction, wavenumber, and the normal derivative are sequentially used in connecting uplink and downlink ray packets over a known surface. From refraction studies and the well-known reciprocity theorem for the Eikonal approximation, there are two unique wavefunctions that are linked in program RD3D from an element of a surface deformed by the missile plume da to the point of observation P on the missile (Fig. 7).

A numerical solution for the net received field due to a disturbance on the surface S can be constructed from Eq. (11) so that the numerical techniques developed for the refraction of EM waves can be incorporated.

In general, if an incoming plane wave is specified as the Green's function, r' is considered large‡ and the inward surface normal is taken such that $\cos(n,r) = -1$, the field at P becomes

$$U_p = \frac{-1}{4\pi}\int_S \frac{e^{ik(r+r')}}{rr'}\left[ik[1+\cos(n,r)] - \frac{1}{r}\cos(n,r)\right]\mathrm{d}a \qquad (12)$$

‡The source is considered at a distance from the surface S, such that the terms $1/r'^2$ can be neglected.

If the distance uplink from the source to the surface S is denoted by r_u and the distance downlink from the surface S to a point of observation P is denoted by r_d such that the uplink and downlink wave paths are partitioned into segments of length dζ and dξ, respectively, the received field at P, U_p, can be represented by the sum

$$U_p = \frac{-1}{4\pi}\sum_i \frac{e^{ik_d r_d}e^{ik_u r_u}}{r_d r_u}\left\{ik_u\left[1+\cos(t_{ui},t_{di}) - \frac{1}{r_d}\cos(t_{ui},t_{di})\right]\right\}\mathrm{d}a_i \qquad (13)$$

where:

$$k_d, r_d = \sum_m (\beta_d + i\alpha_d)\mathrm{d}\xi$$

$$k_u, r_u = \sum_n (\beta_u + i\alpha_u)\mathrm{d}\zeta$$

$$r_d = \sum_m \mathrm{d}\xi$$

$$r_u = \sum_n \mathrm{d}\zeta$$

α_d, β_d = downlink attenuation and phase coefficients

α_u, β_u = uplink attenuation and phase coefficients

and n, m, and i are indexes for uplink, downlink, and surface elements, respectively.

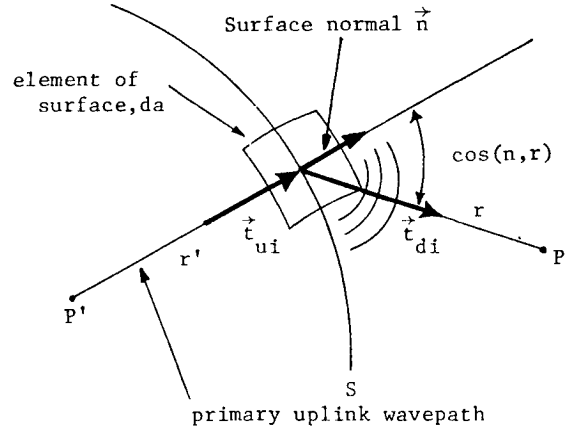

Fig. 6 Geometry for the re-radiation of Huygens' subwavelets contained in the Feesnel-Kirkoff approximation.

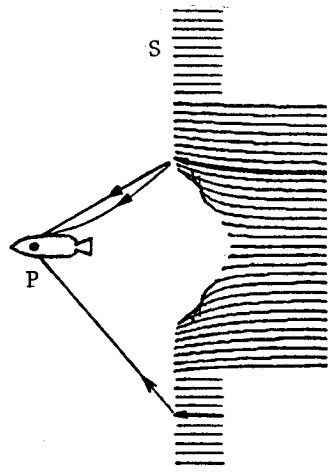

Fig. 7 Integration over the surface S of the Fresnel-Kirkoff equation to a point P on the missile.

Using the computational representation for the net received field, U_p, an arbitrary uplink wave can be propagated in a discrete manner to an element of surface da and repropagated to a point of observation. If care is exercised in the choice of initial wavefunction geometry and transmission vector, the field U_p can be determined from knowledge of the complex wavenumbers, normal derivatives, and position vectors on surface S.

Classical Results

Simple discrete models can be created from classical diffraction theory to confirm the diffraction formulations in RD3D. These predictions may be compared with measured intensity levels from known physical systems. In all cases, Eq. (13), contained in RD3D, is summed over a surface that includes a simple absorbing obstacle that has been substituted for the missile plume.

Experimental results were exhibited for the resultant received intensity due to a slit of fixed width, taken along a line normal to an incoming plane wave at the slit.[15] Numerically performing the sum [Eq. (13)] over the surface of the slit gives results that compare identically with those of Andrews.[15]

Experimental results were also given for the received intensity on the axis of a circular aperture.[15] Once again, Eq. (13) is summed over the surface of the aperture for the experimental arrangement described in Ref. 15. The resultant intensity is illustrated in Fig. 8 for $D/\lambda=2$, where D is the aperture diameter. The result of the numerical integration again compares exactly with experimental data (Ref. 15, Fig. 191, p. 270; Ref. 16).

Subscale Missile Tests

During its development, laboratory measurements were performed by Golden et al.[17] to obtain received EM intensities from various metallic scale models of the Titan IIIC launch vehicle and its plume. The parameters in Ref. 17 describing the experimental apparatus and geometry were employed in program RD3D to model the received EM intensities. The comparison of the experimental data[17] to the numerical model RD3D is depicted in Fig. 9. The experimental data are essentially the effect of diffraction due to an absorbing circular disk and can be analytically solved.[18,19] Figure 10 compares the solution generated from RD3D with the analytical solution.

The numerical model RD3D yields excellent results when compared with simple analytical and experimental models. Without loss of generality, the method of solution is applied to the refracting and diffracting missile plume.

Comparison of RD3D to PK Stage III Data

In order to apply the principles of refraction and diffraction of EM waves through the missile plume, an initial geometry was chosen similar to that depicted in Fig. 7. An uplink three-dimensional plane wave with a circular cross section was chosen as the surface of integration. The plane wave radius was chosen such that the periphery contained unperturbed ray packets. This wave surface was then propagated through the missile plume and integrated over the values of the wavefunction on a surface containing the missile. In order to minimize computational execution time, the numerical integration was performed over just the uplink plane wave with the field outside the circular cross section analytically computed for an opaque circular disk. The application of this technique is known as Babinets' principle.[13,14]

Employing the steady-state plume definition for the PK Stage III rocket motor, the attenuation profile was computed and displayed in Figs. 11 and 12 for missile aspect angles of 0-60 deg for the command and telemetry frequencies of 0.4165 and 2.209 GHz, respectively. During PK flight tests,

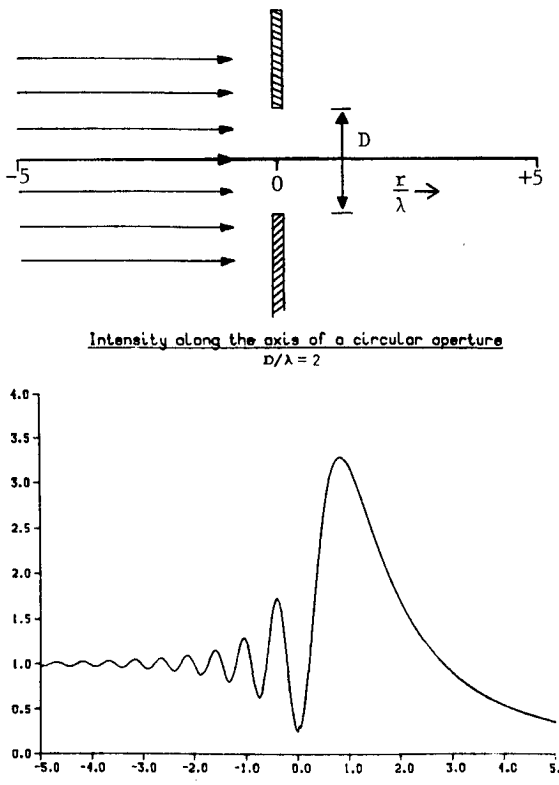

Fig. 8 Resultant intensity due to diffraction through a circular aperture, generalized by program RD3D.

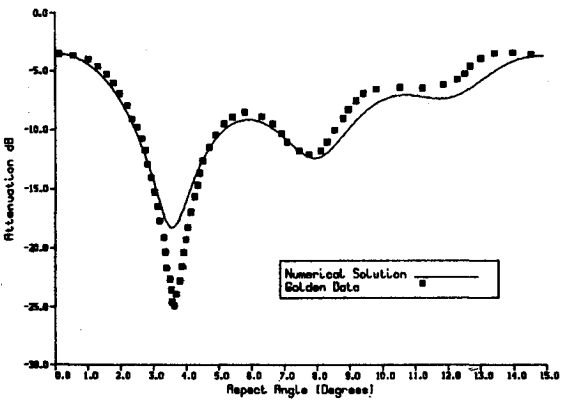

Fig. 9 Comparison of Golden's data and program generated solutions to diffraction about an absorbing circular diffractor.

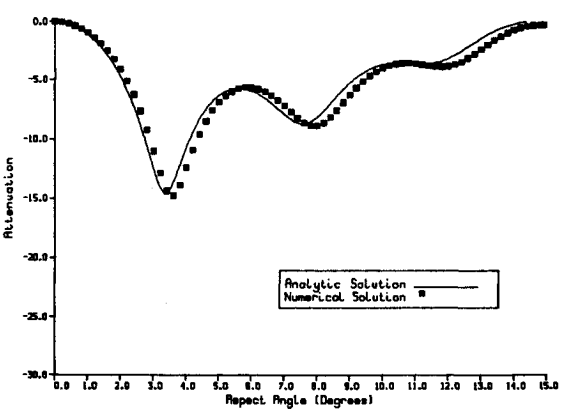

Fig. 10 Comparison of RD3D and analytical circular disk solutions.

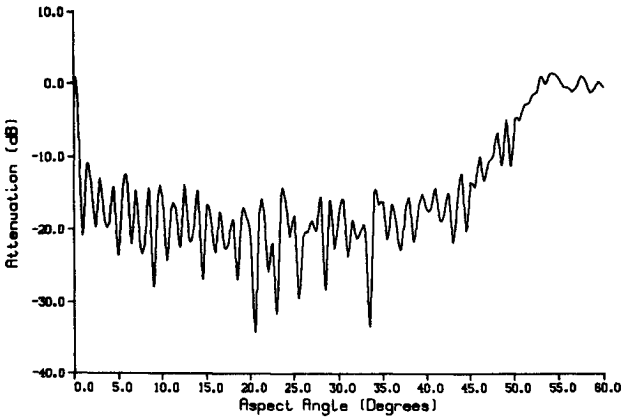

Fig. 11 Received intensity as a function of aspect angle at the command frequency for a plume diffractor as described by Eq. (1).

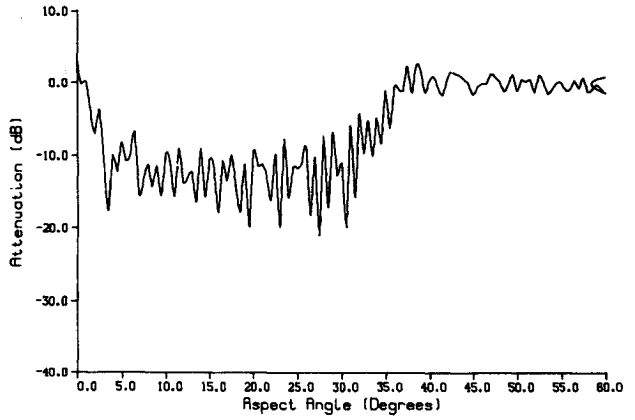

Fig. 12 Received intensity as a function of aspect angle at the telemetry frequency for a plume diffractor as described by Eq. (1).

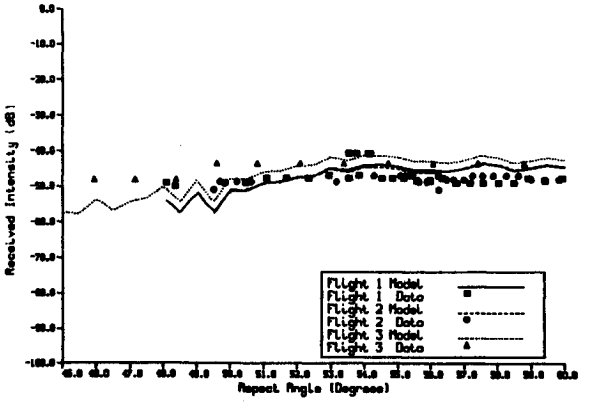

Fig. 13 Comparison of stage III flight data and RD3D solutions for received intensity as a function of aspect angle for command.

measurements of received signal strengths at the command and telemetry frequency were recorded and compared with the model RD3D. Figure 13 compares the data recorded from the first three flight tests with the modeled predictions at the command frequency, and Fig. 14 compares the data recorded from the first two flight tests with predictions for the telemetry frequency. The known space loss, ground system gains, receiver system losses, and the trajectory variation of aspect angle were included in the modeled predictions. An examination of the predicted signal strength intensity at the command frequency shows good agreement in magnitude at higher aspect angles in

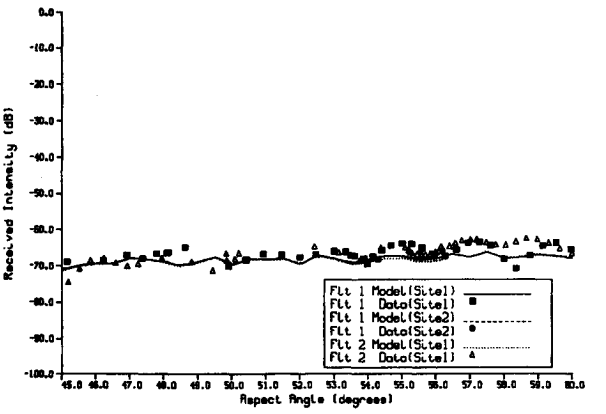

Fig. 14 Comparison of stage III flight data and RD3D solutions for received intensity as a function of aspect angle for telemetry.

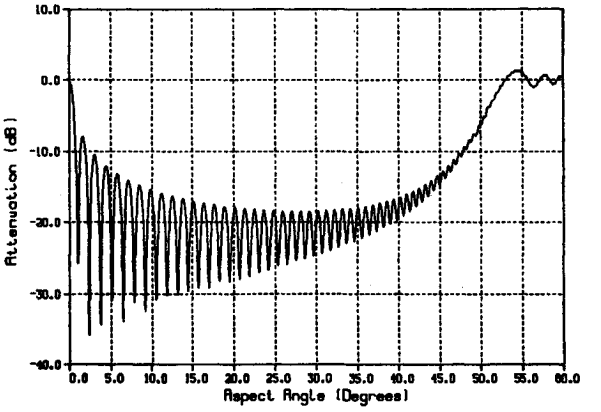

Fig. 15 Analytical circular disk solution applied to an "equivalent diffractor" for stage III.

the 45-60 deg range for stage III. The modeled result tends to deviate from data for aspect angles less than 50 deg. The disparity in comparisons are most likely due to the method by which command data are obtained. For the case of the command frequency data, a "phase center" was chosen for the receiver. In actuality, the real command receiver consists of a pair of slot antennas. The resultant field strengths from one receiver is summed with an unknown component from the other. Phase differences that exist with respect to each receiver would then more likely be apparent at lower aspect angles, where diffraction effects are more prevalent. For the telemetry frequency, a more attractive transmitter and receiver geometry exists. In this case, both the transmitter and receiver can be more accurately treated as "point" sources. Available data show good agreement in trend and magnitude with modeled results for the telemetry frequency.

For highly ionized plumes, the RF interaction with the plume is close to that of an absorbing disk-shaped obstacle. An analytical solution to diffraction about an opaque disk is illustrated in Fig. 15 for the case where similar disk geometries exist with the stage III plume. Figure 11 is then compared with Fig. 15 to point out the similarities of the numerically generated results with an analytical solution. From this comparison, the ionized missile plume is essentially a fuzzy diffractor.

Summary

A computer model has been developed to combine the refractive and diffractive effects of electromagnetic waves through a rocket exhaust plume. Each of the constituent phenomena has been verified with comparison to refraction

studies, classical diffraction results, subscale test results, and the combined field results with full-scale flight test data. Figures showing the distortion of EM waves by refraction illustrate the formation and size of a disk-like diffraction zone. Further, predictions of the net received signal strength by RD3D compare very closely to an analytical model of diffraction around a disk.

References

[1]Coats, D.E. et al., "A Computer Program for the Prediction of Solid Propellant Rocket Motor Performance," AFRPL TR-75-36, Vols. 1-3, July 1975.

[2]Romine, G.L., Senol, A.J., Bryant, R.D., Edquist, C.T., and Huseman, P.G., "RF Signal Degradation from the MX Stage III Plume," Martin Marietta Corp., Technical Operation Rept. SE4-116037, May 1981.

[3]Romine, G.L. and Senol, A.J., "Plume Degradation of RF Signals for MX Stage III and Stage IV," Martin Marietta Corp., Technical Rept. SE4-116076, Sept. 1982.

[4]Curtis, J.T., Moselle, J.R., and Marrone, P.V., "Plume Interference Prediction (PIP) Code: User's Manual and Test and Evaluation Report," Calspan Rept. KC-5900-A-6, Vol. 1, 1977.

[5]Mann, D.M. et al., *JANNAF Rocket Exhaust Plume Technology Handbook,* CPIA Pub. 263, April 1977, Chap. 4.

[6]Bryant, R.D. and Romine, G.L., "Line of Sight RF Signal Degradation due to MX Stage III Rocket Exhaust Plume," Martin Marietta Corp., Technical Operating Rept. SE4-116004, March 1980.

[7]Freehaufer, J.E., "Geometrical Optics," *Propagation of Short Radio Waves,* edited by D.E. Kerr, McGraw-Hill Book Co., New York, 1951, p. 41.

[8]Molmud, P., "RAYBEND—A Ray Tracing Program for Microwaves Propagating Through Rocket Plumes," Paper presented at the JANNAF 12th Plume Technology Meeting, Oct. 1980.

[9]Peng, S.Y., "Analytical Model for Predicting RF Amplitude and Phase Effects of Plume," *JANNAF 10th Plume Technology Meeting,* CPIA Pub. 291, Vol. II, Dec. 1977, p. 1.

[10]Poehler, H.A., "Rocket Exhaust Signal Attenuation and Degradation," Vol. 1, Pan American Aerospace Division, 1969, p. 59.

[11]Taylor, E.C., Vincente, F.A., and Phelps, R.W., "Effects of Rocket Exhausts on Communications Systems," *Proceedings of 4th Space Congress,* Scholarly Publications, Sun Valley, CA, 1967.

[12]Goodman, J.W., *Introduction to Fourier Optics,* McGraw-Hill Book Co., New York, 1968, pp. 33-55.

[13]Jenkins, F.A. and White, H.E., *Fundamentals of Optics,* McGraw-Hill Book Co., New York, 1957.

[14]Jackson, J.D., *Classical Electrodynamics,* John Wiley & Sons, New York, 1975, pp. 427-431, 438.

[15]Andrews, C.L., *Optics of Electromagnetic Spectrum,* Prentice-Hall, Englewood Cliffs, NJ, 1960, pp. 293-295.

[16]Andrews, C.L., "Diffraction Pattern in a Circular Aperture Measured in the Microwave Region," *Journal of Applied Physics,* Vol. 21, 1950, p. 761.

[17]Golden, K.E., Taylor, E.C., and Vincente, F.A., "Diffraction by Rocket Exhausts," IEEE Transactions on Antennas and Propagation, Vol. AP-16, No. 5, Sept. 1968, pp. 614-616.

[18]Gray, A., Matthews, G.B., and Macrobert, T.M., *A Treatise on Bessel Functions and their Applications to Physics,* MacMillan and Co. Ltd., London, 1931.

[19]Senol, A.J., "RF Signal Analysis of the C4-X-21 Trajectory," Martin Marietta Corp., Technical Rept. SE4-116046, Aug. 1981.